

# Physical properties of the layered structure compound $\text{Ce}_3\text{Os}_4\text{Al}_{12}$

RF Djoumessi<sup>1</sup>, BN Sahu<sup>1</sup> and AM Strydom<sup>1</sup>

<sup>1</sup>Highly Correlated Matter Research Group, Physics Department, University of Johannesburg, PO Box 524, Auckland Park 2006, South Africa

E-mail: redrissed@uj.ac.za

**Abstract.** In this work, we report on the structural and physical properties of polycrystalline  $\text{Ce}_3\text{Os}_4\text{Al}_{12}$  synthesized by the argon arc-melting technique. The Rietveld refinement of powder X-ray diffraction patterns confirm that  $\text{Ce}_3\text{Os}_4\text{Al}_{12}$  crystallizes in the hexagonal  $\text{Gd}_3\text{Ru}_4\text{Al}_{12}$ -structure type with space group  $\text{P6}_3/\text{mmc}$ . The temperature dependent dc-magnetic susceptibility and specific heat data reveals that the compound undergoes a ferromagnetic type of ordering below 3 K. The study may contribute towards a better understanding of the physics in distorted Kagomé structure compounds, since in a frustrated lattice system such as this, there are strict constraints imposed upon the occurrence of long-range magnetic order and the magnetic order parameter.

## 1. Introduction

$\text{R}_3\text{T}_4\text{X}_{12}$  type of compounds are of particular interest among intermetallics because the crystal structure contains layers as well as triangular and distorted Kagomé lattice features [1, 2, 3]. The arrangement of the atoms carrying magnetic moments at the vertices of the structure and the competition between ferro- and antiferromagnetic interactions can lead to the appearance of magnetic frustration phenomena. Several studies have been done on Ru-based compounds in this series of aluminides. In these Ru-based compounds, a ferromagnetic behavior is observed in the light rare-earth based compounds (Pr and Nd) [2, 3, 4] while an antiferromagnetic behavior is observed in the heavy rare-earth ones (Gd, Tb, Dy and Yb) [5, 6, 7]. For instance, in  $\text{Gd}_3\text{Ru}_4\text{Al}_{12}$ , geometrical frustration together with the formation of ferromagnetic trimers due to the long-range RKKY interaction is observed at low temperatures [5]. Moreover, a skyrmion lattice with large topological Hall effect has been experimentally observed in the same material [8]. Skyrmions have good potential for information carriers in spintronic devices and frustration is a route towards enhanced skyrmion stability even in systems with a ferromagnetic ground state [9]. In  $\text{Pr}_3\text{Ru}_4\text{Al}_{12}$ , a magnetic moment instability in the presence of crystal electric fields is observed [2]. Despite the number of studies carried out in the  $\text{R}_3\text{Ru}_4\text{Al}_{12}$  series, no physical and magnetic properties have been reported yet on Os-based compounds (except on  $\text{Gd}_3\text{Os}_4\text{Al}_{12}$ ) synthesized for the first time by Niermann [10]. This work is the first report on physical properties of  $\text{Ce}_3\text{Os}_4\text{Al}_{12}$ .

## 2. Synthesis and experimental details

A polycrystalline sample was synthesized by arc-melting stoichiometric amounts of high-purity (99.99 mass % purity or better) elements (Ce, Os and Al) under argon atmosphere in an Edmund Buhler arc-melting furnace. After melting, the sample was annealed in a resistance furnace at 900°C for two weeks and finally water quenched. Dc-magnetic susceptibility, isothermal magnetization and specific heat measurements were performed using a commercial Dynacool physical properties measurement system from Quantum Design, USA. The measurements were carried out in the temperature range between 1.8 K to 300 K and fields up to a maximum value of 9 T.

## 3. Results and Discussion

The powder x-ray diffraction spectrum of this sample (see Fig. 1) was successfully refined on the basis of the hexagonal  $\text{Gd}_3\text{Ru}_4\text{Al}_{12}$  structure type with P63/mmc space group. The structure was refined to  $R_{\text{wp}} = 6.84\%$ ,  $R_{\text{p}} = 4.49\%$  and  $R_{\text{exp}} = 0.98$ . The obtained lattice parameters are  $a = 0.889(1)$  nm and  $c = 0.953(1)$  nm. These values are in good agreement with an earlier report [10]. The refined atomic positions are reported in table 1.

The crystal structure may be described as a layered structure. The Ce atoms occupy only one site in the  $\text{Ce}_3\text{Al}_4$  layer. The Ru atoms share two sites and the Al atoms occupy two different sites in the  $\text{Os}_4\text{Al}_8$  puckered layer (see Fig. 2). The Ce atoms are arranged as a distorted Kagomé net with different sizes of triangles leading to two slightly different nearest-neighbour Ce-Ce distances.

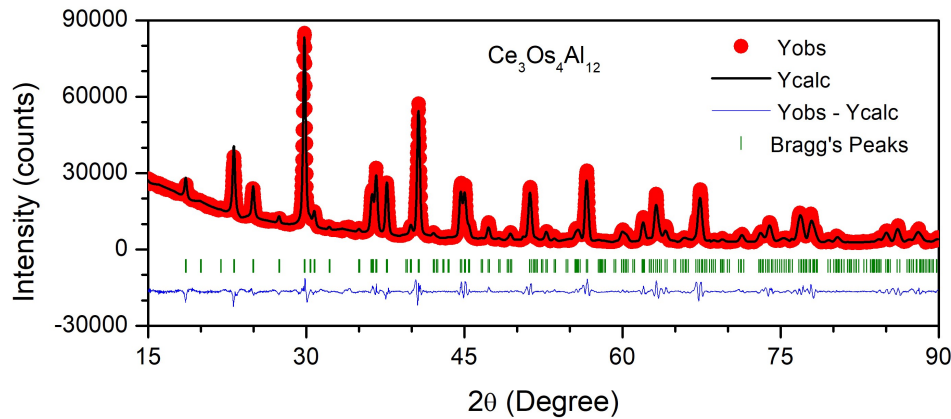


**Figure 1.** (a) Layered representation of the crystal structure of  $\text{Ce}_3\text{Os}_4\text{Al}_{12}$  with Ce (Orange spheres), Os (blue spheres) and Al (green). (b) The  $\text{Ce}_3\text{Al}_4$  layer showing the distorted Kagomé nets.

The main panel of Fig. 3 represents the dc-magnetic susceptibility  $\chi(T)$  of  $\text{Ce}_3\text{Os}_4\text{Al}_{12}$  measured in a magnetic field of 0.1 T. The data are obtained in a field-cooled protocol (cooling of the sample from 300 K to 2 K).  $\chi(T)$  exhibits a modified Curie-Weiss behavior described by equation (1) from 300 K down to 50 K:

$$\chi(T) = \chi_0 + C/(T - \theta_{\text{P}}), \quad (1)$$

where  $\chi_0$  is the temperature independent susceptibility,  $C$  is the Curie-Weiss constant, and  $\theta_{\text{P}}$  is the paramagnetic Weiss temperature. From the least-squares fit of equation (1) to the data, we obtained an effective magnetic moment ( $\mu_{\text{eff}}$ ) of  $0.54 \mu_{\text{B}}/\text{Ce}$  ion which is less than one quarter

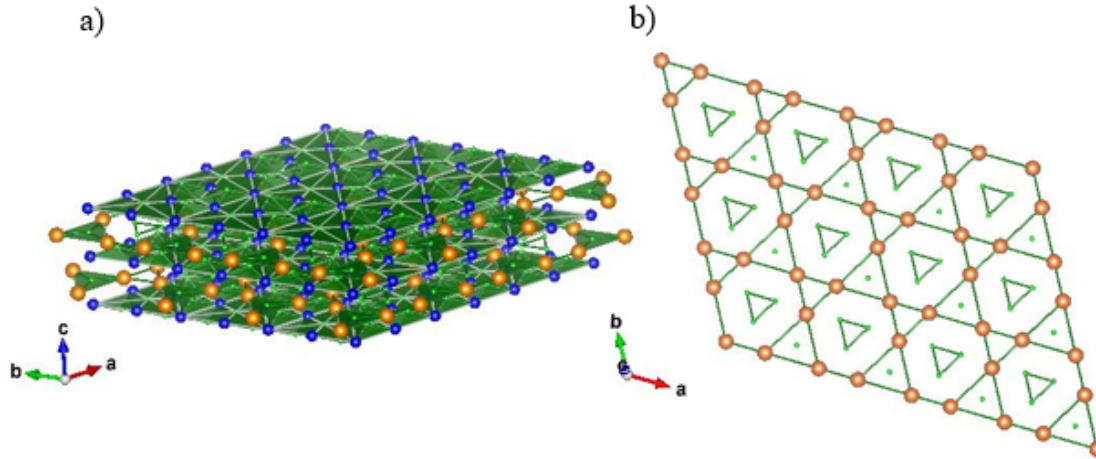


**Figure 2.** (a) Layered representation of the crystal structure of Ce<sub>3</sub>Os<sub>4</sub>Al<sub>12</sub> with Ce (Orange spheres), Os (blue spheres) and Al (green). (b) The Ce<sub>3</sub>Al<sub>4</sub> layer showing the distorted Kagomé nets.

**Table 1.** Crystallographic details of Ce<sub>3</sub>Os<sub>4</sub>Al<sub>12</sub>.

Atom	Wyckoff	x	y	z	Occupancy
Ce	6h	0.19174	0.38348	0.25000	0.19211
Os <sub>1</sub>	6g	0.50000	0.00000	0.00000	0.30492
Os <sub>2</sub>	2a	0.00000	0.00000	0.00000	0.11893
Os <sub>3</sub>	6h	0.00000	0.00000	0.25000	0.11893
Al <sub>1</sub>	12k	0.16523	0.33046	0.57419	0.42748
Al <sub>2</sub>	6h	0.53125	0.12953	0.25000	0.02533
Al <sub>3</sub>	4f	0.33333	0.66667	0.02753	0.19764
Al <sub>4</sub>	2b	0.00000	0.00000	0.25000	0.05803

of the theoretical value of a free trivalent Ce ion ( $2.54 \mu_B$ ) in Ce<sub>3</sub>Os<sub>4</sub>Al<sub>12</sub>. This suggests either an itinerant character or a strong crystal field effect of the 4f-electrons in Ce<sub>3</sub>Os<sub>4</sub>Al<sub>12</sub>. The paramagnetic Weiss temperature is found to be  $\theta_P = +5.3$  K with the positive sign indicating the dominance of ferromagnetic interactions in the high temperature region. The kink observed around the transition temperature  $T_c = 3$  K (see inset (a) of Fig. 3) is a sign of a short-range order-like transition. Isothermal magnetization at temperatures between 2 K and 20 K is presented in the inset (b) of Fig. 3. Broad curvatures are observed below 6 K. The saturation magnetization at 2 K and in 9 T is only about  $0.06 \mu_B/\text{Ce}$  ion which is less than 5% of the full saturation value compared to the free ion saturation value  $2.16 \mu_B/\text{Ce}$ . The quasi-linear behavior above 6 K indicates a paramagnetic state.

The main panel of Fig. 4 represents the specific heat of Ce<sub>3</sub>Os<sub>4</sub>Al<sub>12</sub> and La<sub>3</sub>Os<sub>4</sub>Al<sub>12</sub> as function of temperature. The high temperature region resembles the behavior of a normal metal. Inset (a) of Fig 4 represents the low-temperature region. The blue symbols represent the magnetic 4f contribution to the specific heat obtained by subtracting the specific heat of La<sub>3</sub>Os<sub>4</sub>Al<sub>12</sub> from that of Ce<sub>3</sub>Os<sub>4</sub>Al<sub>12</sub>. The kink observed around the transition temperature  $T_c = 3$  K is a sign of a short-range order-like transition. Inset (b) shows the 4f contribution to the entropy per Ce as a function of temperature. The magnetic contribution released at  $T_c$  is about  $0.6 \text{ J/mole}_{\text{Ce}} \cdot \text{K}^2$  which is about 10% of the value  $R \ln 2$  expected for a doublet ground

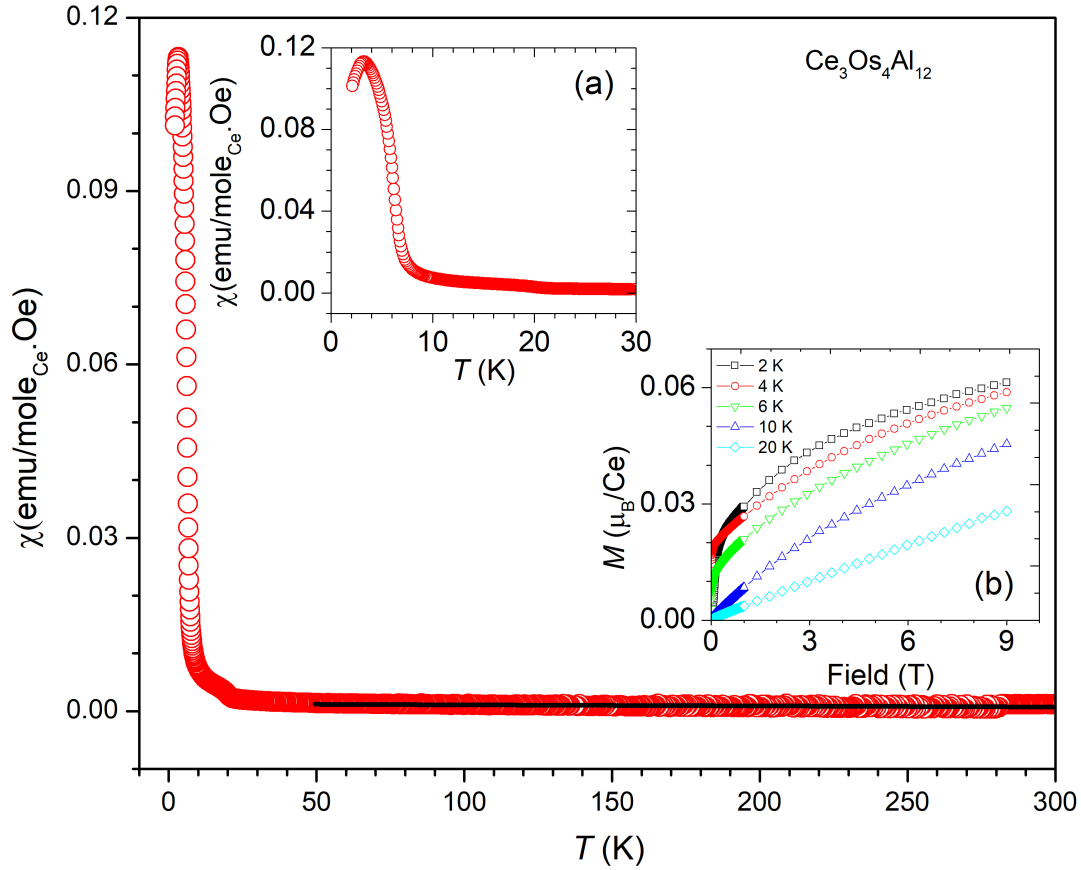


**Figure 3.** Main panel: magnetic susceptibility of  $\text{Ce}_3\text{Os}_4\text{Al}_{12}$  measured in a constant de-magnetic field of 0.1 T. The black line represents the least-squares fit of the modified Curie-Weiss relation (see equation 1). Inset (a) highlights the low-temperature region. Inset (b) represents the isothermal magnetization at temperatures between 2 K and 20 K.

state of the crystal field split multiplet of trivalent Ce. Inset (c) of Fig 4 represents the specific heat  $C_{4f}(T)/T$  vs  $T^2$ .  $C_{4f}(T)/T$  at  $T \rightarrow 0$  reaches  $0.4 \text{ J/mol}_{\text{Ce}} \cdot \text{K}^2$  which is enhanced by a factor of 100 above that of an ordinary metal [11]. This points to a large residual 4f-electron entropy in the low-temperature limit which is likely caused by strong electron correlations in the Ce compound.

#### 4. Conclusion

$\text{Ce}_3\text{Os}_4\text{Al}_{12}$  is a new example of a layered distorted Kagomé structure with possible effects of the geometric frustration. The  $\chi(T)$  and  $C_p(T)$  data confirm the presence of weak magnetic order. Further magnetic studies are needed to describe in detail the nature of the phase transition observed in  $\text{Ce}_3\text{Os}_4\text{Al}_{12}$ .

##### 4.1. Acknowledgments

RFD thanks OWSD and SIDA for fellowships towards her PhD studies. B. Sahu thanks Global Excellence and Stature (UJ-GES) fellowship, University of Johannesburg. AMS thanks the URC/FRC of UJ and the SA-NRF (93549) for financial support.

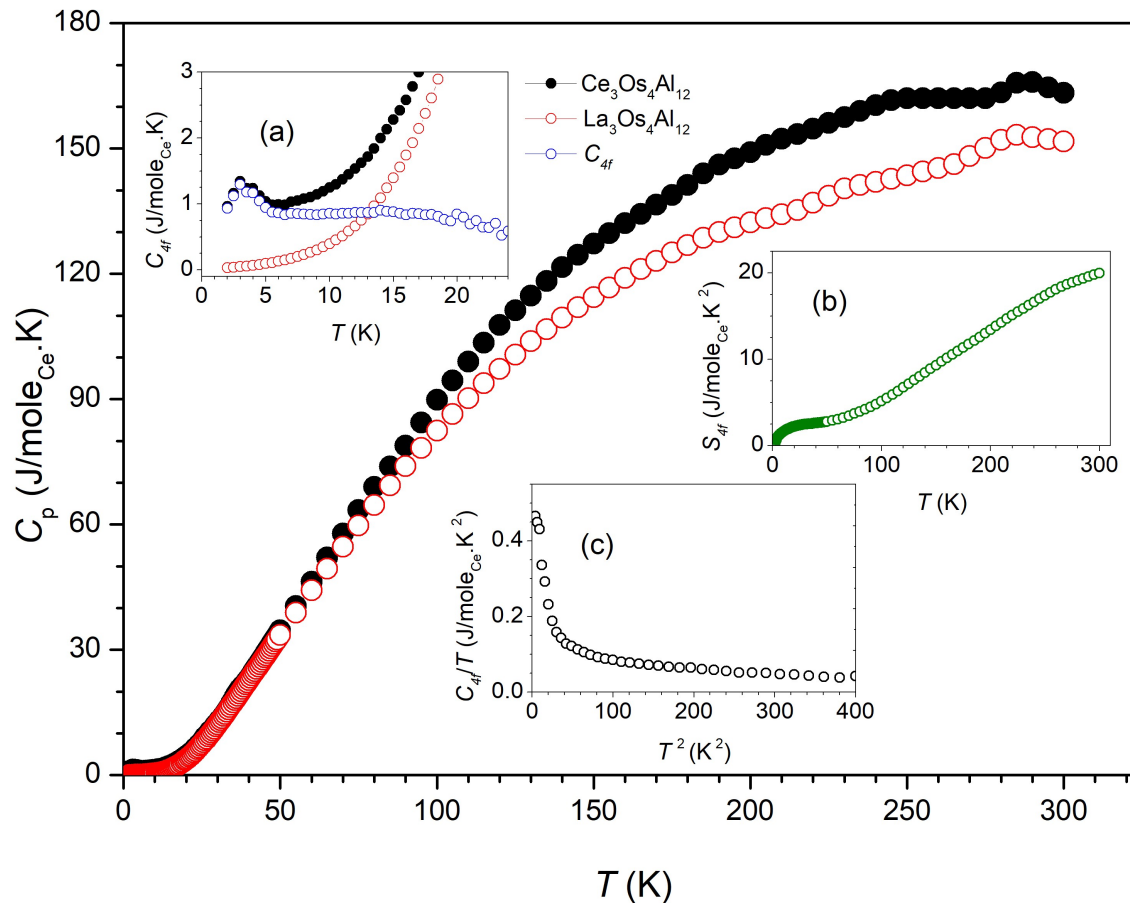


**Figure 4.** Main panel: Specific heat of  $\text{Ce}_3\text{Os}_4\text{Al}_{12}$  and  $\text{La}_3\text{Os}_4\text{Al}_{12}$  against temperature. Inset (a) represents the low-temperature region. The blue symbols represent the 4f-electron contribution to the specific heat of  $\text{Ce}_3\text{Os}_4\text{Al}_{12}$  obtained by subtracting the specific heat of  $\text{La}_3\text{Os}_4\text{Al}_{12}$  from that of  $\text{Ce}_3\text{Os}_4\text{Al}_{12}$ . Inset (b) shows the 4f contribution to the entropy per Ce as a function of temperature. Inset (c) illustrates  $C_{4f}(T)/T$  vs  $T^2$ .

## References

- [1] Ge W, Michioka C, Ohta H and Yoshimura K 2014 *Solid State Communications* **195** 1–5
- [2] Henriques M, Gorbunov D, Andreev A, Fabrèges X, Gukasov A, Uhlarz M, Petříček V, Ouladdiaf B and Wosnitza J 2018 *Physical Review B* **97** 014431
- [3] Gorbunov D, Henriques M, Andreev A, Gukasov A, Petříček V, Baranov N, Skourski Y, Eigner V, Paukov M and Prokleška J 2014 *Physical Review B* **90** 094405
- [4] Gorbunov D, Henriques M, Andreev A, Eigner V, Gukasov A, Fabrèges X, Skourski Y, Petříček V and Wosnitza J 2016 *Physical Review B* **93** 024407
- [5] Nakamura S, Kabeya N, Kobayashi M, Araki K, Katoh K and Ochiai A 2018 *Physical Review B* **98** 054410
- [6] Upadhyay S K, Iyer K K and Sampathkumaran E 2017 *Journal of Physics: Condensed Matter* **29** 325601
- [7] Nakamura S, Toyoshima S, Kabeya N, Katoh K, Nojima T and Ochiai A 2015 *Physical Review B* **91** 214426
- [8] Hirschberger M, Nakajima T, Gao S, Peng L, Kikkawa A, Kurumaji T, Kriener M, Yamasaki Y, Sagayama H and Nakao H 2019 *Nature Communications* **10** 1–9
- [9] Von Malottki S, Dupé B, Bessarab P F, Delin A and Heinze S 2017 *Scientific Reports* **7** 1–10
- [10] Niermann J and Jeitschko W 2002 *Zeitschrift für anorganische und allgemeine Chemie* **628** 2549–2556
- [11] Kittel C, McEuen P and McEuen P 1996 *Introduction to Solid State Physics* vol 8 (Wiley New York)